Applicability of perturbative QCD and NLO power corrections for the pion form factor

Tsung-Wen Yeh
Institute of Physics, National Chiao-Tung University, Hsinchu, Taiwan 300, Republic of China
(Received 4 September 2001; revised manuscript received 7 January 2002; published 19 March 2002)

As is well recognized, the asymptotic of the perturbative QCD prediction for the pion form factor is much smaller than the upper end of the data. We investigate this problem. We first evaluate the next-to-leading-order (NLO) power correction for the pion form factor. The corrected form factor contains nonperturbative parameters which are determined from a χ^2 fit to the data. Interpreting these parameters leads to the fact that the involved strong interaction coupling constant should be identified as an effective coupling constant under a nonperturbative QCD vacuum. If the scale associated with the effective coupling constant is identified as $\langle x\rangle^2 Q^2$, then Q^2, the momentum transfer square for the pion form factor to be measured, can have a value about 1 GeV^2, and $\langle x\rangle$, the averaged momentum fraction variable, can locate around 0.5. This circumstance is consistent with the asymptotic model for the pion wave function.

DOI: 10.1103/PhysRevD.65.074016 PACS number(s): 12.38.Bx, 13.40.Gp

I. INTRODUCTION

The exclusive process plays an important role in improving our understanding of strong interactions. A detailed analysis of the exclusive process may exhibit the constituents of hadrons and shed light on the underlying dynamics. One important progress in this respect is that perturbative QCD (PQCD) was proposed for exclusive processes involving large momentum transfer [1–5]. The basic idea of PQCD in these processes is the factorization theorem, which demonstrates that the transition amplitude can be factorized into a convolution of hadronic wave functions and a hard function. The hard function involving the short-distance interactions is perturbatively calculable, while the hadronic wave functions containing the long-distance physics are nonperturbative. PQCD has the ability to predict outcome due to the fact that for a specific hadron, its hadronic wave function is universal for transition processes in which the hadron can participate.

The pion form factor has been investigated in the framework of PQCD [4–15]. In the experimentally accessible energy region of a few GeV^2, the asymptotics of PQCD is only about one-fourth of the experimental value. This fact has received much attention in the literature. It also stimulated the debate about whether PQCD can be used for the pion form factor. As indicated by Isgur and Llewellyn [16,17], most contributions to the form factor are from the soft end-point regions, i.e., the end-point singularity with which the perturbative calculation would become unreliable. To resolve this problem, Li and Sterman [6] proposed a modified hard-scattering approach for the hadronic form factor. In this approach, the end-point singularity is replaced by a resummation over soft radiative corrections, i.e., the Sudakov form factor. It was found that, with the transverse degrees of freedom playing the role of infrared cutoff, the PQCD contribution becomes self-consistent for momentum transfer as low as a few GeV. Other approaches to solve the end-point singularity problem have also been proposed, such as the transverse structure of the pion wave function [18–20], the effective gluon mass [21], and the frozen running coupling constant [22,23].

The discrepancy between theory and experiment may be eliminated by power correction [10–12,15] or radiative correction. However, as shown in [7,8], the next-leading-order (NLO) radiative corrections can only contribute 20–30 %, which is still not enough to account for the data. Therefore, it is interesting to find out how large a contribution the NLO power correction can give. For the pion form factor, the NLO [i.e., $O(1/Q^4)$] power correction may receive contributions from operators composed either of one twist-2 and one twist-4 distribution amplitude (DA) or two twist-3 DAs [24]. The contributions from the latter have been calculated in PQCD [10–12,15]. To have a complete PQCD description for the form factor up to NLO power correction, the contributions from the former must also be considered. Based on the method developed in [25], the former type of operator can be systematically calculated. The most important feature of this method is that the NLO power correction can have a partonic interpretation. By combining the contributions from both types of operators, we can find an interpretation for the data.

The organization of this paper is as follows. We investigate the power expansion for the $\gamma^*\pi\to\pi$ process in Sec. II. The pion form factor $F_\pi(Q^2)$ up to order $O(Q^{-4})$ is evaluated in Sec. III. Using the pion form factor, we arrive at a phenomenological pion form factor by employing a least-χ^2 fit to the data. Comparisons between the theoretical and the phenomenological pion form factors are given. Section IV contains discussions and conclusions.

II. COLLINEAR EXPANSION

In this section, we shall describe our approach for the power expansion for the $\gamma^*\pi\to\pi$ process. The method we shall employ is called the collinear expansion [25–27]. Let $\sigma=\phi^*(P_2,k_2)\otimes\sigma_p(k_1,k_2)\otimes\phi(P_1,k_1)$ represent the lowest-order amplitude for $\gamma^*(q)\pi(P_1)\to\pi(P_2)$ as depicted in Fig. 1(a). The explicit form for the amplitude σ is expressed as

$$\sigma=\int\frac{d^4k_1}{(2\pi)^4}\frac{d^4k_2}{(2\pi)^4}\mathrm{Tr}[\phi^*(k_2)\sigma_p(k_1,k_2)\phi(k_1)],\quad(1)$$

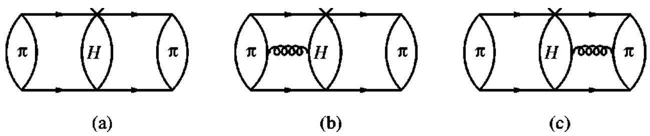

FIG. 1. The leading diagrams for $\gamma^*\pi\to\pi$.

where $\sigma_p(k_1,k_2)$ denotes the amplitude for the partonic subprocess, and $\phi(k_i)$, $i=1,2$, represents the pion DAs. The $\otimes$ denotes convolution integrals over the loop momenta k_i and traces over the color indices and the spin indices. To pick out the leading contribution, we assign the momenta of the initial- and final-state pions in the following way. We choose $P_1=(P_1^+,P_1^-,P_{1\perp})=(Q/\sqrt{2},0,\mathbf{0}_\perp)$ and $P_2=(P_2^+,P_2^-,P_{2\perp})=(0,Q/\sqrt{2},\mathbf{0}_\perp)$ such that PQCD is applicable for $Q^2=-q^2=-(P_2-P_1)^2$ being large. We shall employ the light-cone gauge in the following calculations. The internal loop momenta k_i^μ, $i=1,2$, are parametrized as

$$k_i^\mu=x_iP_i^\mu+\frac{k_i^2+k_{i\perp}^2}{2x_i}n_i^\mu+k_{i\perp}^\mu, \tag{2}$$

where x_i are dimensionless numbers of order unity and the vectors n_i are in the direction of the opposite-moving external vectors such that $n_i\cdot P_i=1$, $n_i^2=0$, $n_1\cdot n_2=2/Q^2$, and also $n_1\cdot P_2=n_2\cdot P_1=0$. The first step is to perform a Taylor expansion for the partonic amplitude

$$\sigma_p(k_i)=\overline{\sigma}_p(k_i=x_iP_i)+(\overline{\sigma}_p)_\alpha(x_i,x_i)w^\alpha_{i\alpha'}k_i^{\alpha'}+\cdots, \tag{3}$$

where we have assumed the low-energy theorem

$$\frac{\partial}{\partial k^{\alpha_i}}\sigma_p(k_i)\bigg|_{k_i=x_iP_i}=(\overline{\sigma}_p)_\alpha(x_i,x_i) \tag{4}$$

and have employed $w^\alpha_{i\alpha'}k_i^{\alpha'}=(k_i-x_iP_i)^\alpha$ and $w^\alpha_{i\alpha'}=g^\alpha_{\alpha'}-P_i^\alpha n_{i\alpha'}$. The leading term $\phi^*\otimes\overline{\sigma}_p\otimes\phi$ contains leading, next-to-leading, and even higher-order power corrections which should be determined from the spin structure of $\overline{\sigma}_p$, the term proportional to $\not{n}_i$ or $\not{P}_i$. The $\not{n}_i$ term would project a collinear $q\overline{q}$ pair from the meson, while the $\not{P}_i$ term would not diminish only when the $q\overline{q}$ pair carries noncollinear momenta. The second step is to substitute the leading partonic amplitude $\overline{\sigma}_p$ into the convolution integral with the pion wave function ϕ to factorize the leading and subleading power contributions,

$$\phi^*\otimes\overline{\sigma}_p\otimes\phi=\phi_0^*\otimes\overline{\sigma}_p\otimes\phi_0+\phi_0^*\otimes\overline{\sigma}_p\otimes\phi_1+\phi_1^*\otimes\overline{\sigma}_p\otimes\phi_0+\cdots, \tag{5}$$

where ϕ_0 and ϕ_1 denote the leading twist (LT) and next-to-leading twist (NLT) pion DAs, respectively. The ϕ_1 contains both short-distance and long-distance contributions. The short-distance contributions of ϕ_1 arise from the noncollinear components of k_i. By the equation of motion, the noncollinear components of k_i will induce one quark-gluon vertex $i\gamma_\alpha$ and one special propagator $i\not{n}_i/2x_i$ [27]. Because the special propagator is not propagating on the light cone associated with the meson, the quark-gluon vertex and the special propagator should be incorporated into the hard function, $\overline{\sigma}_p$. In this way, ϕ_1 is factorized into $\phi_1\approx(\phi_1^H)_\alpha w^\alpha_{1\alpha'}(\phi_{1,D})^{\alpha'}$ and the short-distance piece $(\phi_1^H)_\alpha$ is absorbed into $\overline{\sigma}_p$. This leads to the third step,

$$\begin{aligned}\phi_0^*\otimes\overline{\sigma}_p\otimes\phi_1&=\phi_0^*\otimes\overline{\sigma}_p\otimes[(\phi_1^H)_\alpha\bullet w^\alpha_{1\alpha'}(\phi_{1,D})^{\alpha'}]\\&=\phi_0^*\otimes(\overline{\sigma}_p\bullet\phi_1^H)_\alpha\otimes w^\alpha_{1\alpha'}(\phi_{1,D})^{\alpha'},\end{aligned} \tag{6}$$

where $(\phi_{1,D})^{\alpha'}$ containing the covariant derivative $D^{\alpha'}=i\partial^{\alpha'}-gA^{\alpha'}$ is implied. The related Feynman diagrams for this type of correction are displayed in Fig. 2. In these diagrams, the quark propagator with one bar denotes the special propagator.

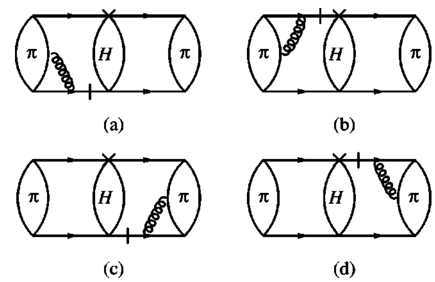

FIG. 2. The NLO power correction diagrams for $\gamma^*\pi\to\pi$. The propagator with one bar means the special propagator.

We now describe the final step of the collinear expansion. The second term of Eq. (3) can contribute in subleading order of the power correction as it convolutes with ϕ_0. The momentum factor k^α is absorbed by ϕ_0 to become a coordinate derivative, denoted as $k^\alpha\phi_0\equiv\phi^\alpha_{1,\partial}$. Consider the other contributions $\sigma_1\approx\phi_0^*\otimes(\overline{\sigma}_p)_\alpha\otimes w^\alpha_{1\alpha'}\phi^{\alpha'}_{1,A}$ from Fig. 1(b), where $\phi^\alpha_{1,A}$ contains gauge fields. Because of color and electromagnetic gauge invariance, the diagrams from Fig. 3 are necessary. Note that the term $w^\alpha_{1\alpha'}A^{\alpha'}$ appears automatically in the light-cone gauge. To arrive at a final result, some care should be taken. There are two kinds of contributions. The contributions of the first kind are from those diagrams in which the pion DAs contain the covariant derivative. We can set these as

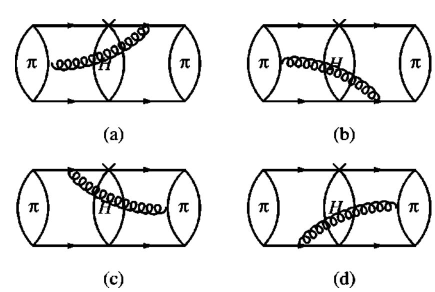

FIG. 3. The other NLO power correction diagrams for $\gamma^*\pi\to\pi$.

$$\phi_0^* \otimes (\overline{\sigma}_p)_\alpha \otimes w_{1\alpha'}^\alpha \phi_{1,\partial}^{\alpha'} + \phi_0^* \otimes (\overline{\sigma}_p)_\alpha \otimes w_{1\alpha'}^\alpha \phi_{1,A}^{\alpha'} \equiv \phi_0^* \otimes (\overline{\sigma}_p)_1 \otimes (\phi_{1,D}), \tag{7}$$

where we have employed $\phi_{1,\partial}^\alpha + \phi_{1,A}^\alpha = \phi_{1,D}^\alpha$. The contributions of the other kind are from those diagrams in which the DAs contain only gluon fields. Because of gauge invariance, the gluon fields need to be converted into field strengths. That is, we need to make the following substitution for the gluon field:

$$A^\alpha \to \frac{1}{y} G^{\alpha\beta} n_{1\beta}, \tag{8}$$

where the gluon field is associated with momentum yP_1 and the factor $1/y$ is then absorbed by the corresponding partonic amplitude $(\overline{\sigma}_p)_\alpha$ such that $(\overline{\sigma}_p)_\alpha \to (\overline{\sigma}_p^G)_\alpha$. These contributions are expressed as

$$\phi_0^* \otimes (\overline{\sigma}_p^G)_\alpha \otimes w_{1\alpha'}^\alpha \phi_{1,G}^{\alpha'} \equiv \phi_0^* \otimes (\overline{\sigma}_p^G)_1 \otimes (\phi_{1,G}), \tag{9}$$

where $\phi_{1,G}^\alpha$ means that it contains $G^{\alpha\beta}$. The last two steps of the collinear expansion can be applied for the final-state pion to calculate the other contributions. Finally, we write the amplitude of the process $\gamma^* \pi \to \pi$ under the collinear expansion up to $O(1/Q^4)$ as

$$\begin{aligned} \sigma_0 + \sigma_1 \approx\, & \phi_0^* \otimes \overline{\sigma}_p \otimes \phi_0 \\ & + \phi_0^* \otimes [\overline{\sigma}_p \bullet \phi_1^H + (\overline{\sigma}_p)_1] \otimes \phi_{1,D} \\ & + \phi_{1,D}^* \otimes [(\phi_1^{*H}) \bullet \overline{\sigma}_p + (\overline{\sigma}_p)_1^*] \otimes \phi_0 + \phi_0^* \otimes (\overline{\sigma}_p^G)_1 \\ & \otimes \phi_{1,G} + \phi_{1,G}^* \otimes (\overline{\sigma}_p^G)_1^* \otimes \phi_0 . \end{aligned} \tag{10}$$

Where NLT DAs $\phi_{1,D}$ and $\phi_{1,G}$ are involved in the NLO power correction.

The remaining tasks to be considered are the factorizations of the spin indices, the color indices, and the momentum integrals over the loop partons. We refer the reader to [25] for details of these factorizations. For factorization of spin indices, we employ the expansion of the meson DA into its spin components as

$$\phi_{0,1} = \sum_\Gamma \phi_{0,1}^\Gamma \Gamma, \tag{11}$$

where Γ denotes the Dirac matrix $\Gamma = 1, \gamma^\mu, \gamma^\mu\gamma_5, \sigma^{\mu\nu}$, and ϕ_1 represents $\phi_{1,D}$ or $\phi_{1,G}$. The choice of the lowest twist components $\phi_{0,1}^\Gamma$ of $\phi_{0,1}$ can be made by employing power counting [25]. For the factorization of the color indices, we employ the convention that the color indices of the parton amplitudes are extracted and attributed to the meson DAs. The factorization of the momentum integral is performed by making use of the fact that the leading parton amplitudes depend only on the momentum fraction variables x_i. The momentum integrals are then converted into the integrals over fraction variables.

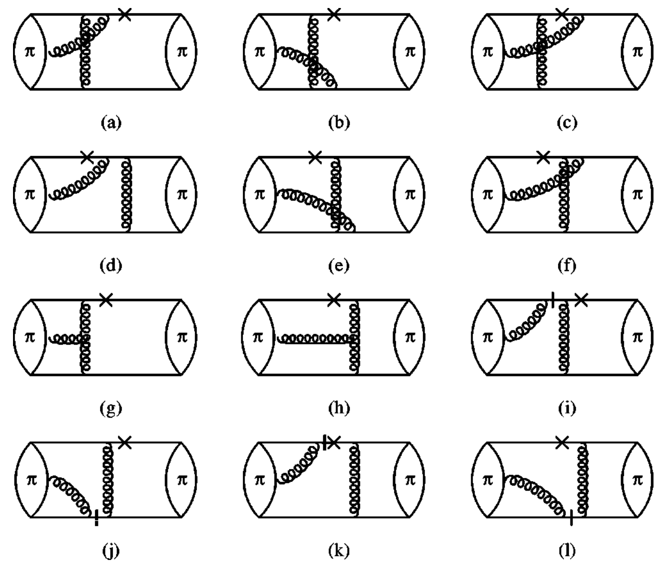

FIG. 4. The leading NLO power correction diagrams for $\gamma^*\pi \to \pi$. The Hermitian conjugate diagrams are implied.

III. $O(Q^{-4})$ CONTRIBUTIONS

The amplitude for the $\gamma^*\pi\to\pi$ process can be parametrized in terms of the pion form factor,

$$A(\gamma^*\pi\to\pi) = -ie_\pi F_\pi(Q^2)(P_1^\mu + P_2^\mu), \tag{12}$$

where $Q^2 = (P_2 - P_1)^2$ denotes the virtuality of the off-mass-shell photon and e_π is the pion charge. The leading contribution of the pion form factor $F_\pi(Q^2)$ is expressed as

$$F_\pi^{\rm LO}(Q^2) = \frac{128\pi\alpha_s(Q_{\rm eff}^2)}{9Q^2} \int_0^1 dx \int_0^1 dy \frac{\phi(x)\phi(y)}{xy}. \tag{13}$$

Applying $\phi(x) = 3 f_\pi x(1-x)/\sqrt{2}$ into Eq. (13), one can get

$$F_\pi^{\rm LO}(Q^2) = \frac{16\pi\alpha_s(Q_{\rm eff}^2) f_\pi^2}{Q^2}, \tag{14}$$

where $f_\pi = 93$ MeV will be used below in the numerical analysis.

We now describe the calculations of the NLO power correction. We shall employ the light-cone gauge. The leading Feynman diagrams displayed in Fig. 4 are considered. After explicit evaluations for each diagram, we find the nonvanishing contribution is from Fig. 4(d). The result then reads

$$F_\pi^{\rm NLO}(Q^2) = -\frac{256\pi\alpha_s(Q_{\rm eff}^2)}{9Q^4} \times \int_0^1 dx \int_0^1 dy \frac{[G(x) + \tilde{G}(x)]\phi(y)}{x^2 y} + (x \leftrightarrow y), \tag{15}$$

where $G(x)$ and $\tilde{G}(x)$ denote twist-4 pion DAs [25]. To simplify the situation further, we assume that $G(x)$ and $\tilde{G}(x)$

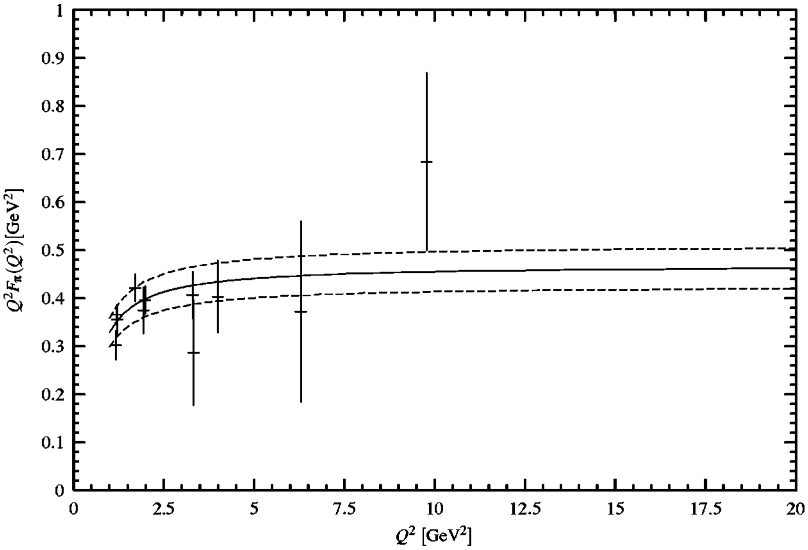

FIG. 5. Plot of the least χ^2 fit (solid line) and C.L.=99.73% (dash line) for $Q^2F_\pi(Q^2)$. The experimental data are taken from [1–3].

contribute equally. A remark for the calculation is that we have employed the spin tensors $i\epsilon_\perp^{\alpha\beta}\gamma_\beta$ for $G(x)$ and $d_\perp^{\alpha\beta}\gamma_\beta\gamma_5$ for $\tilde{G}(x)$, where $\epsilon_\perp^{\alpha\beta}=\epsilon^{\alpha\beta\gamma\lambda}P_{1\gamma}n_{1\lambda}$ and $d_\perp^{\alpha\beta}=P_1^\alpha n_1^\beta+n_1^\alpha P_1^\beta-g^{\alpha\beta}$.

We have employed the effective coupling $\alpha_s(Q^2_{\rm eff})$ with the argument $Q^2_{\rm eff}\equiv\langle xyQ^2\rangle$, where the brackets denote the average under a nonperturbative QCD vacuum. This is contrary to the usual approach in PQCD, in which $\alpha_s(Q^2)$ is taken to be running with Q^2. The scale xyQ^2 of α_s is chosen as the momentum transfer of the exchanged gluon. From the factorization point of view, we may incorporate $\langle xyQ^2\rangle$ into $\langle x\rangle\langle y\rangle Q^2_{\rm fact}$ by a factorization scale $Q_{\rm fact}$, which denotes a scale to separate the perturbative and nonperturbative dynamics. After substituting $G(x)=3\sqrt{2}\pi^2f_\pi^3x(1-x)$ [25] and evaluating the integrals, there still remains an infrared divergence [10,28]

$$F_\pi^{\rm NLO}(Q^2)=-\frac{512\pi^3f_\pi^4\alpha_s(Q^2_{\rm eff})}{Q^4}\left(\int\frac{(1-x)}{x}dx\right) \quad (16)$$

which is from on-shell quark lines. This divergence cannot be completely resolved under perturbation theory. There requires a resummation over the soft divergences associated with the virtual quark lines. One also needs to introduce a jet function to absorb these divergences. We shall skip the detailed perturbative structure of these divergences [10–12,28]. The initial function for such a jet function is nonperturbative. We denote the jet function as $J(Q^2_{\rm eff})$ and reset the NLO form factor as

$$F_\pi^{\rm NLO}(Q^2)=-\frac{512\pi^3f_\pi^4\alpha_s(Q^2_{\rm eff})J(Q^2_{\rm eff})}{Q^4}. \quad (17)$$

Combining $F_\pi^{\rm LO}(Q^2)$ and $F_\pi^{\rm NLO}(Q^2)$, we obtain

$$F_\pi(Q^2)=\frac{16\pi\alpha_s(Q^2_{\rm eff})f_\pi^2}{Q^2}\left(1-\frac{32\pi^2f_\pi^2J(Q^2_{\rm eff})}{Q^2}\right)+O(Q^{-6}). \quad (18)$$

Inspired by the above theoretical pion form factor, we can perform a least-χ^2 ($\chi^2_{\rm min}$=7.967 42) fit to the data [1–3] to obtain a phenomenological form factor,

$$F_\pi^{\rm fit}(Q^2)=\frac{A}{Q^2}\left(1-\frac{B}{Q^2}\right), \quad (19)$$

where $A=0.468\,95^{+0.042\,53}_{-0.043\,29}$ with 6σ accuracy and $B=0.3009$. The χ^2 analysis for the data is shown in Fig. 5. It is obvious that the data point at 10 GeV^2 is the result of allowed errors. However, due to a small available range of Q^2 for the data, it is difficult to determine the asymptotic of the scaled form factor $Q^2F_\pi(Q^2)$ at large Q^2. Comparing Eqs. (18) and (19), we are led to the following conclusions.

(i) The argument of $\alpha_s(Q^2)$ should be interpreted as an effective $Q^2_{\rm eff}\equiv\langle x\rangle^2Q^2_{\rm fact}$. That is, we need to take $\alpha_s(Q^2)$ as an effective coupling constant. The average fraction has the value $\langle x\rangle\approx0.57\pm0.03$ for $Q_{\rm fact}=1$ GeV and $\Lambda_{\rm QCD}=0.3$ GeV. The values of $\langle x\rangle$ and $Q^2_{\rm fact}$ depend on the model for the pion DA [the asymptotic (AS) model]. If we perform a similar analysis by employing the Chernyak-Zhitnitsky (CZ) model $\phi(x)=15f_\pi x(1-x)(1-2x)^2/\sqrt{2}$ and $G(x)=15\sqrt{2}\pi^2f_\pi^3x(1-x)(1-2x)^2$ [25], we can have $Q^2_{\rm fact}=13.12^{+5.79}_{-3.39}$ GeV^2 for $\langle x\rangle\approx0.5$ or $Q^2_{\rm fact}=32.8^{+14.5}_{-8.5}$ GeV^2 for $\langle x\rangle\approx0.1$. It is clear that the CZ model is less consistent with PQCD than the AS model.

(ii) A less model-dependent property of the effective coupling constant can be described. The change in $\Lambda_{\rm QCD}$ would affect the location of the average fraction variable $\langle x\rangle$ for a fixed factorization scale $Q_{\rm eff}$. On the other hand, for a fixed $\langle x\rangle$, $Q_{\rm eff}$ would vary with $\Lambda_{\rm QCD}$. Nevertheless, there only exist finite possible consistent solutions for $\Lambda_{\rm QCD}$, $Q_{\rm eff}$, and $\langle x\rangle$.

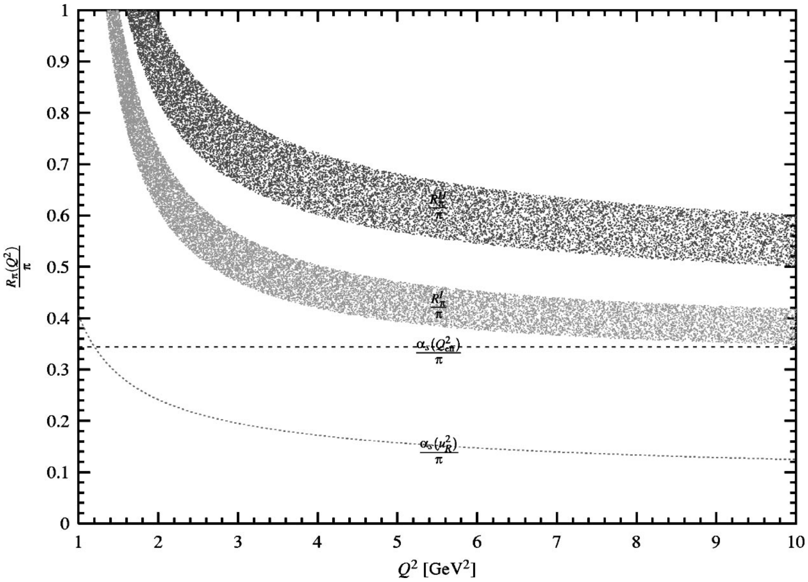

FIG. 6. The comparisons between R_π^I/π, R_π^{II}/π, $\alpha_s(\mu_R^2)/\pi$, and $\alpha_s(Q^2_{\rm eff})/\pi$.

(iii) The effective value of the J function at $Q^2_{\rm eff}$ is also model-dependent with a value of about 0.11 for the AS model and 0.026 for the CZ model.

(iv) Because the pion-photon transition form factor $F_{\pi\gamma}(Q^2)$ up to $O(1/Q^4)$ takes the form [25]

$$F_{\pi\gamma}(Q^2)=\frac{2f_\pi}{Q^2}\left(1-\frac{8\pi^2 f_\pi^2}{Q^2}\right), \qquad (20)$$

it is interesting to define the ratio R_π [5],

$$R_\pi^I(Q^2)=\frac{F_\pi^{\rm fit}(Q^2)}{4\pi Q^2 F^2_{\pi\gamma}(Q^2)}, \qquad (21)$$

which has a theoretical expression valid for $Q^2 \geqslant 1\ GeV^2$,

$$R_\pi^I(Q^2)=\alpha_s(Q^2_{\rm eff})\left(1+\frac{16\pi^2 f_\pi^2[1-2J(Q^2_{\rm eff})]}{Q^2} -\frac{64\pi^4 f_\pi^4}{Q^4}+O(1/Q^6)\right). \qquad (22)$$

Comparing the prediction of $F_{\pi\gamma}$ in Eq. (20) with the data [29] gives $\chi^2=12.8$ for 15 data points. Note that the $F_{\pi\gamma}$ in Eq. (20) is multiplied by 5/3 if the CZ model for the pion DAs has been employed. The ratio R_π^I is then smaller by 9/25. However, it has been shown [25] that the data [29] for the $F_{\pi\gamma}$ form factor are more suited to the AS model than the CZ model, because the result with CZ DAs has $\chi^2=390$ (see the Fig. 3 in [25]). Since Eq. (20) is close to the experiment, we may take it as a fit to the data. The ratio $R_\pi^I(Q^2)$ is a ratio of observable over observable.

As the pion-photon transition form factor with the NLO correction, which has the expression

$$F^{\rm as}_{\pi\gamma}(Q^2)=\frac{2f_\pi}{Q^2}\left(1-\frac{5}{3}\,\frac{\alpha_s(\mu_R^2)}{\pi}\right) \qquad (23)$$

with $\mu_R^2=Q^2/9$, can also explain the data ($\chi^2=57.8$), we can define a similar ratio

$$R_\pi^{II}(Q^2)=\frac{F_\pi^{\rm fit}(Q^2)}{4\pi Q^2[F^{\rm as}_{\pi\gamma}(Q^2)]^2} \qquad (24)$$

whose expression reads

$$R_\pi^{II}(Q^2)=\alpha_s(Q^2_{\rm eff})\left(1+\frac{10}{3}\,\frac{\alpha_s(\mu_R^2)}{\pi}-\frac{25}{9}\,\frac{\alpha_s^2(\mu_R^2)}{\pi^2} -\frac{32\pi^2 f_\pi^2 J(Q^2_{\rm eff})}{Q^2}+O(\alpha_s^3)\right). \qquad (25)$$

The $F^{\rm as}_{\pi\gamma}(Q^2)$ in Eq. (23) is calculated by the AS model for the leading twist pion DA and the usual one-loop formula for the QCD running coupling constant,

$$\alpha_s(Q^2)=\frac{4\pi}{\beta_0 \ln\frac{Q^2}{\Lambda^2_{\rm QCD}}}, \qquad (26)$$

where $\Lambda_{\rm QCD}=0.2$ GeV and $\beta_0=11-2/3n_f$ with $n_f=2$ have been used. We compare $R_\pi^I(Q^2)/\pi$ and $R_\pi^{II}(Q^2)/\pi$ in Fig. 6. The errors for the ratios $R_\pi^{I(II)}$ are from the errors associated with the fit pion form factor $F_\pi^{\rm fit}$. Also plotted are $\alpha_s(Q^2_{\rm eff})/\pi$ and $\alpha_s(\mu_R^2)/\pi$ employed in $F^{\rm as}_{\pi\gamma}$. From Fig. 6, $R_\pi^{I(II)}$ are larger than $\alpha_s(\mu_R^2)$ by about a factor of 3–5. The difference between R_π and α_s cannot be compensated for even by including the experimental errors for the $F_{\pi\gamma}$ form factor, which can enlarge the error range for R_π by 100%. This seems to indicate that the other effects we have not considered may be important. For example, we can encounter two possibilities: the NLO correction and the effects of QCD coupling in the low momentum region. The NLO correction can give contributions of at most 10% [see point (V)]. As for the QCD coupling in the low momentum region, which can be modeled by an effective charge [30],

$$\alpha_V(Q^2)=\frac{4\pi}{\beta_0\frac{Q^2+m_g^2}{\Lambda_V^2}} \tag{27}$$

with nonperturbative parameters Λ_V and m_g being a few hundred MeVs, still cannot account for the large value of R_π. However, due to the low quality of the available data for the pion form factor, it is difficult to draw a firm conclusion regarding the above discrepancy between experiment and theory. We expect that future experiment could support further evidence to resolve the above problem.

(V) By taking into account the contributions from the $O(\alpha_s^2)$ corrections to the leading twist pion form factor [31], Eq. (18) is then modified as

$$F_\pi(Q^2)=\frac{16\pi\alpha_s(Q_{\rm eff}^2)f_\pi^2}{Q^2}\left\{1+\frac{\alpha_s(Q_{\rm eff}^2)}{\pi}\left[\frac{\beta_0}{4}\left(\ln\frac{1}{18}+\frac{14}{3}\right)-3.92\right]\right\}\left(1-\frac{32\pi^2f_\pi^2J(Q_{\rm eff}^2)}{Q^2}\right)+O(Q^{-6}). \tag{28}$$

The maximum values of the NLO α_s corrections have been taken [31]. With the $O(\alpha_s^2)$ corrections, it only amounts to reinterpreting the scale $Q_{\rm eff}$ involved in the coupling constant $\alpha_s(Q_{\rm eff}^2)$. The value of the jet function is unchanged. This can be seen from the expression of $F_\pi^{\rm fit}(Q^2)$, where the expansion is strictly ordered in $1/Q^2$. The analysis for $Q_{\rm eff}$ is close to that described in point (i) within 5%. The $O(\alpha_s^2)$ correction for the ratio R_π can also be considered by directly applying Eq. (28). We find that the effects of the $O(\alpha_s^2)$ correction for R_π are about 5–10 %. Of course, the complete $O(\alpha_s^2)$ corrections are still not available. The analysis made here only reflects partial effects and seems too simple.

IV. DISCUSSIONS AND CONCLUSIONS

We now estimate the percentage of perturbation contributions to the pion form factor. Our approach is to extend the analysis of Isgur *et al*. by including the NLO power correction. The analysis of Isgur *et al*. estimates the perturbation contributions of the pion form factor by employing the fractional function $f(\epsilon)$

$$f(\epsilon)=\int_0^1dx\int_0^1dy\ \theta(xy-\epsilon)\frac{\phi(x)\phi(y)}{xy}. \tag{29}$$

The parameter ϵ describes a cutoff on xy in order to keep higher-twist contributions and higher-order effects at a reasonably small level. The reference scale is chosen at 1 GeV. Since $f(\epsilon)$ is a mixture of perturbative and nonperturbative contributions, the perturbation parts are those corresponding to large values of xyQ^2. For the AS model, $f(\epsilon)$ reaches 90% for $\epsilon=1/150$. This implies that the naive perturbative contribution is 90% accurate for $Q^2=150\ \ {\rm GeV}^2$. As for the pion form factor with NLO power corrections, the function $f(\epsilon)$ is modified, accordingly, as

$$f(\epsilon^{\rm NLO})=\int_0^1dx\int_0^1dy\,\theta(xy-\epsilon^{\rm NLO})\frac{\phi(x)\phi(y)}{xy}, \tag{30}$$

where $\epsilon^{\rm NLO}=\epsilon(1-c)$ with $c=0.3009$. It is easy to find that $f(\epsilon^{\rm NLO})$ reaches 90% for $\epsilon^{\rm NLO}=1/150$ or $\epsilon=1/105$. This means that the perturbative contribution with NLO power corrections is 90% accurate for $Q^2=105\ \ {\rm GeV}^2$. One may see that the inclusion of NLO power corrections can really improve the range of perturbation contributions by about 30%. As for the CZ model, the analysis can be made to reach a similar conclusion.

We now analyze the effects of the NLO power corrections from the operators composed in terms of two twist-3 pion DAs [10–12,15]. This type of NLO power correction takes the expression

$$F_\pi^{\rm NLO}(Q^2)=\frac{16\pi\alpha_s(Q^2)f_\pi^2m_\pi^4}{Q^4m_0^2}J^2(Q^2). \tag{31}$$

The function $J(Q^2)$ is the jet function as introduced before. The factor m_π^2/m_0 relates to the quark condensate $\langle 0|\bar{q}q|0\rangle$ as

$$\frac{m_\pi^2}{m_0}=-\frac{2}{f_\pi^2}\langle 0|\bar{q}q|0\rangle. \tag{32}$$

Using the standard value of the quark condensate $\langle 0|\bar{q}q|0\rangle(1\ \ {\rm GeV})=(-240\ \ {\rm MeV})^3$, one has $m_\pi^2/m_0\approx 1.56$ GeV in comparison with $(16\pi^2f_\pi^2)^{1/2}\approx 1.17$ GeV. By substituting $\alpha_s(Q^2)$ by $\alpha_s(Q_{\rm eff}^2)$ and $J(Q^2)$ by $J(Q_{\rm eff}^2)$ in Eq. (31) and adding Eq. (31) into Eq. (18), we can arrive at

$$F_\pi(Q^2)=\frac{16\pi\alpha_s(Q_{\rm eff}^2)f_\pi^2}{Q^2}\left(1-\frac{32\pi^2f_\pi^2}{Q^2}J(Q_{\rm eff}^2)+\frac{m_\pi^4}{Q^2m_0^2}J^2(Q_{\rm eff}^2)\right)+O(Q^{-6}). \tag{33}$$

This implies that the value of the jet function, $J(Q_{\rm eff}^2)\approx 0.124$, is changed by about 10%. It is obvious that Eq. (31) is as important as Eq. (18).

It is instructive to check whether the Sudakov form factor can compete with the NLO power correction. The Sudakov form factor arises when one performs a resummation over the soft radiative gluons [5,6]. For the pion form factor, the associated Sudakov form factor behaves like

$$\exp\left[-\frac{8C_F}{\beta_0}\ln\left(\frac{Q^2}{\Lambda^2}\right)\ln\left(\frac{\ln(Q^2/\Lambda^2)}{\ln(k_\perp^2/\Lambda^2)}\right)\right]$$
$$=\left(\frac{\Lambda^2}{Q^2}\right)^{(8C_F/\beta_0)\ln[\ln(Q^2/\Lambda^2)/\ln(k_\perp^2/\Lambda^2)]}, \qquad (34)$$

where $k_\perp$ is the transverse momentum of the loop momentum and Λ represents Λ_{QCD}, and we have used $C_F=\frac{4}{3}$. It is seen that the Sudakov form factor at $k_\perp\approx\Lambda$, where the power expansion makes sense, decreases faster than any power suppression for $Q^2>\Lambda^2$. Therefore, the Q^2 behavior of the pion form factor at moderate Q^2 is mainly controlled by the power correction.

We have developed a power expansion scheme for $\gamma^*\pi\to\pi$. The NLO power correction to the pion form factor has been calculated. By employing the form of the pion form factor with NLO power correction, we then perform a least-χ^2 analysis for the data to derive a phenomenological pion form factor. By comparing the phenomenological and the theoretical form factors, we arrive at the conclusion that, due to the nonperturbative QCD vacuum, the strong-coupling constant should be identified as an effective coupling constant with a factorization scale equal to 1 GeV. In addition, the averaged fraction variable is located at 0.5 in agreement with the AS model for the pion DA. The CZ model fails to give a consistent explanation for the data, because its relative factorization scale is in the range of 3–7 GeV.

From the results of this paper and [25], we see that the power correction for exclusive processes is not negligible and requires detailed investigations. Over past decades, we have accumulated abundant data for exclusive processes. Most data are in the low-energy region, which is where the power correction plays an important role. The leading or the asymptotic contribution only gives information about the hadronic wave function, the static property of QCD, while the power correction can reveal the dynamics of QCD.

ACKNOWLEDGMENTS

This work was supported in part by the National Science Council of R.O.C. under Grant No. NSC89-2811-M-009-0024.

[1] C.J. Bebek *et al.*, Phys. Rev. Lett. **37**, 1525 (1976).
[2] C.J. Bebek *et al.*, Phys. Rev. D **17**, 1693 (1978).
[3] NA7 Collaboration, S.R. Amendolia *et al.*, Nucl. Phys. **B277**, 168 (1986).
[4] G.P. Lepage and S.J. Brodsky, Phys. Lett. **87B**, 359 (1979).
[5] G.P. Lepage and S.J. Brodsky, Phys. Rev. D **22**, 2157 (1980).
[6] H. Li and G. Sterman, Nucl. Phys. **B381**, 129 (1992).
[7] R.D. Field, R. Gupta, S. Otto, and L. Chang, Nucl. Phys. **B186**, 429 (1981).
[8] B. Melic, B. Nizic, and K. Passek, Phys. Rev. D **60**, 074004 (1999).
[9] A.V. Efremov and A.V. Radyushkin, Phys. Lett. **94B**, 245 (1980).
[10] B.V. Geshkenbein and M.V. Terentev, Phys. Lett. **117B**, 243 (1982).
[11] B.V. Geshkenbein and M.V. Terentev, ITEP-45-1982.
[12] B.V. Geshkenbein and M.V. Terentev, Yad. Fiz. **40**, 758 (1984) [Sov. J. Nucl. Phys. **40**, 487 (1984)].
[13] V.L. Chernyak and A.R. Zhitnitsky, Phys. Rep. **112**, 173 (1984).
[14] R. Jakob and P. Kroll, Phys. Lett. B **315**, 463 (1993); **319**, 545(E) (1993).
[15] F. Cao, Y. Dai, and C. Huang, Eur. Phys. J. C **11**, 501 (1999).
[16] N. Isgur and C.H. Llewellyn Smith, Phys. Rev. Lett. **52**, 1080 (1984).
[17] N. Isgur and C.H. Llewellyn Smith, Nucl. Phys. **B317**, 526 (1989).
[18] T. Huang and Q.X. Shen, Z. Phys. C **50**, 139 (1991).
[19] Z. Dziembowski and L. Mankiewicz, Phys. Rev. Lett. **58**, 2175 (1987).
[20] F.G. Cao, T. Huang, and B.Q. Ma, Phys. Rev. D **53**, 6582 (1996).
[21] C.R. Ji, A.F. Sill, and R.M. Lombard, Phys. Rev. D **36**, 165 (1987).
[22] C.R. Ji and F. Amiri, Phys. Rev. D **42**, 3764 (1990).
[23] J.M. Cornwall, Phys. Rev. D **26**, 1453 (1982).
[24] V.M. Braun, A. Khodjamirian, and M. Maul, Phys. Rev. D **61**, 073004 (2000).
[25] T. Yeh, hep-ph/0107018.
[26] R.K. Ellis, W. Furmanski, and R. Petronzio, Nucl. Phys. **B207**, 1 (1982).
[27] J. Qiu, Phys. Rev. D **42**, 30 (1990).
[28] H. Li, hep-ph/0102013.
[29] CLEO Collaboration, J. Gronberg *et al.*, Phys. Rev. D **57**, 33 (1998).
[30] S.J. Brodsky, C.R. Ji, A. Pang, and D.G. Robertson, Phys. Rev. D **57**, 245 (1998).
[31] B. Melic, B. Nizic, and K. Passek, hep-ph/9908510.